Journal of the Ceramic Society of Japan 123 [4] 268-273 2015 Paper

Three electrode configuration measurements of electrolyte-diffusion barrier-cathode interface

Dagmara SZYMCZEWSKA, Jakub KARCZEWSKI,* Aleksander CHRZAN and Piotr JASIŃSKI†

Faculty of Electronics, Telecommunications and Informatics, Gdansk University of Technology, 80–233 Gdańsk, ul. Narutowicza 11/12 Poland
***Faculty of Applied Physics and Mathematics, Gdansk University of Technology, 80–233 Gdańsk, ul. Narutowicza 11/12 Poland**

Measurements of a system consisting of cathode/doped ceria diffusion barrier/doped zirconia electrolyte were made using two- and three-electrode configuration. Results obtained on a three-electrode measurement configuration were compared with and reflect the results obtained in two-electrode configuration. Three-electrode measurements allowed separating the impact of the symmetrical interface in the investigated system. They also enabled to obtain additional information about the investigated interface, such as the behavior of the system under an external polarization voltage. It has been shown that the 200 to 1200 nm thick CGO diffusion barrier layer fabricated by spray pyrolysis significantly reduces the polarization resistance of the interface. It also minimizes the impact of the polarization resistance in the presence of external polarization voltage.

Key-words : Three electrode measurement, Reference electrode, Diffusion barrier layer, SOFC, CGO

[Received February 2, 2015; Accepted February 21, 2015]

1. Introduction

These days solid oxide fuel cells (SOFCs) are widely investigated energy converters.[1] Taking into account a growing interest of clean energy production,[2] the future of the SOFCs is very promising. Currently, the state of the art SOFC is fabricated using yttria stabilized zirconia as an electrolyte, $(La,Sr)(Co,Fe)O_3$ perovskite family as a cathode and Ni-cermet as an anode.[3),4] It is known that these cathodes chemically react with YSZ electrolyte. This leads to formations of low conductive phases, i.e. $La_2Zr_2O_7$ and $SrZrO_3$, due to cations diffusion during the cell fabrication and operation.[5),6] These phases formed at the interface of cathode and electrolyte increase the fuel cell ohmic and polarization losses and decrease its overall performance.[7] To prevent formation of low conductive phases, a diffusion barrier interlayer is usually fabricated at the cathode/electrolyte interface. Promising results have been obtained when the lanthanum-strontium based cathode and the YSZ electrolyte have been separated by a gadolinium doped cerium oxide (CGO) layer. The fuel cells having CGO barrier layers and $La_{1-x}Sr_xCo_{1-y}Fe_yO_{3-\delta}$ cathodes have shown better performance and stability overtime.[8] CGO exhibit high oxide ion conductivity, inertness towards both lanthanum-strontium based cathodes and YSZ electrolyte as well as chemical stability under cell operating conditions.[9] An ideal diffusion barrier should be thin, dense and allow fabrication by a fast, cost-efficient, and up-scalable process. For thin layer fabrication very promising is a spray pyrolysis method, which enables the cost effective production of dense and homogeneous layers without requiring high temperatures. Application of spray pyrolysis for fabrication diffusion barrier helps avoiding the problem of the CGO and YSZ solid solution formation, which exists in case of the application of conventional methods requiring sintering at above 1200°C.[9]

As indicated above, the knowledge about interactions between the layers is the key issue for the fuel cell efficiency improvement. Commonly, these interactions are investigated by the measurement of cell overpotentials using impedance spectroscopy.[10] Frequently, this type of test is performed on symmetrical cells having two identical electrodes on both sides of the electrolyte.[11] As a result of such test the obtained information provides the total overpotential. In order to estimate the information about each interface the overpotential is divided by two.[11] This indirect method of testing electrode overpotentials allows examination of only one kind of interface. A study of the unsymmetrical cells, e.i. the cells having different type of an anode and a cathode, provides information about the total overpotential and usually does not allow the separation of the individual interface impacts. To be able to pull out this information, the system should be equipped with an additional reference electrode and measured in potentiostatic configuration. The investigated interface (SOFC anode or cathode) should be connected to the working electrode, while the opposite electrode to the counter electrode of the potentiostat. Such a measurement configuration, refered to as three-electrode configuration, provides an additional advantage of the interface investigation in a condition, which simulates the operating condition of a fuel cell. Namely, it is possible to apply a bias voltage during testing,[11] which allows investigation of working electrode overpotential behavior in conditions existing during fuel cell operation. In order to obtain reliable results in measurements with three-electrode configuration, the location of the reference electrode is not arbitrary.[12] Moreover, the working and the counter electrode should occupy the same area on opposite sides of the electrolyte, and should not be shifted relative to each other.[13),14] The reference electrode should be located at the area where the potential distribution is uniform and constant.[15),16] In addition, the reference electrode should be

† Corresponding author: P. Jasiński; E-mail: piotr.jasinski@eti.pg.gda.pl
‡ Preface for this article: DOI http://dx.doi.org/10.2109/jcersj2.123.P4-1

DOI http://dx.doi.org/10.2109/jcersj2.123.268

positioned at a distance greater than the triple thickness of the electrolyte from the edge of the working and counter electrode,[14),17)] while its size should not be too large.[18),19)]

In this study gadolinia-doped ceria buffer layers were fabricated using spray pyrolysis methods. The influence of the CGO buffer layer thickness was evaluated. In order to characterize the effect of the buffer layer both a two- and three-electrode configuration measurements were performed. It has been demonstrated that alike results can be obtained on system with two- and three-electrode configuration. Moreover, the cathode overpotentials were investigated under bias conditions, what reflects the conditions under the fuel cell operation.

2. Experimental

Three sets of structures with CGO barrier layer have been evaluated. Namely, symmetrical structures (for two-electrode configuration measurements) and symmetrical and asymmetrical structures with reference electrode (for three-electrode configuration measurements) were fabricated and investigated. The symmetrical structures, which are frequently used for SOFC cathode overpotential evaluation, were prepared to validate the measurements obtained on three-electrode symmetrical structures. The investigated structures were built on the yttria stabilized zirconia (YSZ) supports. In order to prepare supports YSZ powder (Tosoh) was pressed into pellets under the pressure of 45 MPa and sintered at 1400°C for 2 h. Obtained pellets had a thickness of 0.85 mm and a diameter of 12.6 mm. A diffusion barrier made of gadolinium-doped ceria was deposited on YSZ pellets by a spray pyrolysis method. The liquid precursor was prepared from $Ce(NO_3)_3{\cdot}6H_2O$ (Sigma-Aldrich, 99%) and $Gd(NO_3)_3{\cdot}6H_2O$ (Sigma-Aldrich, 99.9%) dissolved in water, polyethylene glycol and tetraethylene glycol (Sigma-Aldrich 99%). The precursor was sprayed (airbrush Paasche VL) onto the YSZ substrate heated to a temperature of 440°C. The flow of precursor was adjusted to obtain film growing rate of 200 nm/h. The deposited film was annealed at 900°C. Gadolinium-doped ceria films with a thickness of 200, 400, 800, 1200 nm were prepared. In order to ensure the high quality of the films, the layers with a thickness greater than 400 nm were deposited in a multistep process. A single step process involves deposition of 400 nm thick layer and annealing at 900°C. In the multistep procedure, a single step was repeated until the desired thickness was obtained. On the CGO deposited layers, a LSF ($La_{0.6}Sr_{0.4}FeO_{3-\delta}$) cathode (100 µm thick) was brush painted. Prepared structure was sintered at 1100°C. In order to elucidate the influence of the electrode surface area on obtained results, the structures with the LSF diameters of 0.3, 0.5, 0.7 and 0.9 cm were prepared and investigated. A platinum current collector was applied on LSF cathode by brush painting of the ESL 5545 (Electroscience Laboratory) paste and annealing at 900°C.

The schematic diagrams of investigated structures are presented in **Fig. 1**. In case of the two-electrode symmetrical structures [see Fig. 1(a)] all of the layers were deposited symmetrically on both sides of the electrolyte. The three-electrode symmetrical structures [see Fig. 1(b)] were prepared similarly with the only difference that the platinum reference electrode was attached to the edge of the pellet. The reference electrode was always (apart from the largest electrode diameter of 0.9 cm) away from the working electrode by a distance greater than triple the thickness of the electrolyte. According to the literature, this is the minimum distance to obtain reliable results in three-electrode configuration.[14),17)] Also three-electrode asymmetrical structures were prepared, which structure is schematically depicted in Fig. 1(c). The asymmetric sample had the investigated layers on the only one side of the YSZ support (working electrode), while on the opposite side a platinum was placed (counter electrode). Also, in each configuration (two-electrode symmetrical and three-electrode symmetrical and asymmetrical), the structures without CGO layer were prepared for a reference.

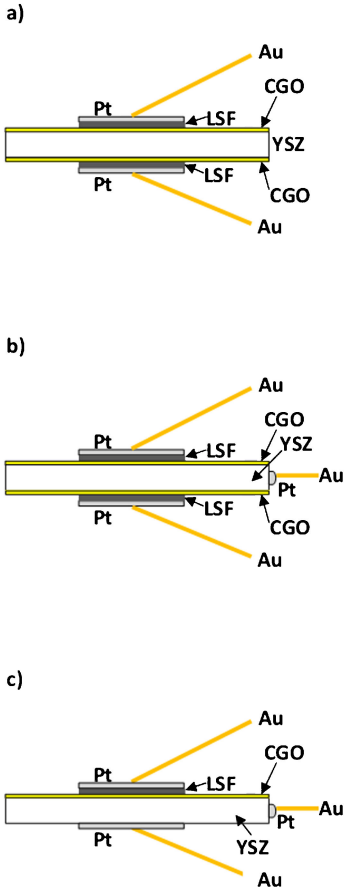

Fig. 1. Diagram showing samples arrangement for two-electrode configuration (a), three-electrode symmetrical configuration (b) and three-electrode asymmetrical configuration (c).

Electrical measurements were carried using an impedance analyzer Solartron SI 1260 combined with a potentiostat/galvanostat Solartron SI 1287. Measurements were performed in the frequency range from 1 MHz to 0.5 Hz with a voltage excitation of 20 mV in the temperature range 600–800°C. The cross section images of cathode-electrolyte interface were investigated by scanning electron microscopy (FEI QUANTA FEG 250).

3. Results and discussion

The cross-section scanning electron microscopy images of an electrolyte-cathode interface area are presented in **Fig. 2**. The interface of the structure without CGO diffusion barrier layer is presented in Fig. 2(a). It is visible in this image that a dense layer of about 0.5 µm thick is formed between electrolyte and LSF cathode. This layer was identified by the EDX detector as strontium-zirconate phase. It seems that the diffusion of strontium from the LSF cathode into the electrolyte is rather extensive at the annealing temperature of 1100°C. The cross-section images of the structures with the CGO diffusion barrier layer of 400, 800 and 1200 nm are presented in Figs. 2(b)–2(d), respectively. The expected thickness of the CGO layer nearly accurately reflects the actual layer thickness, while the multistep approach of the

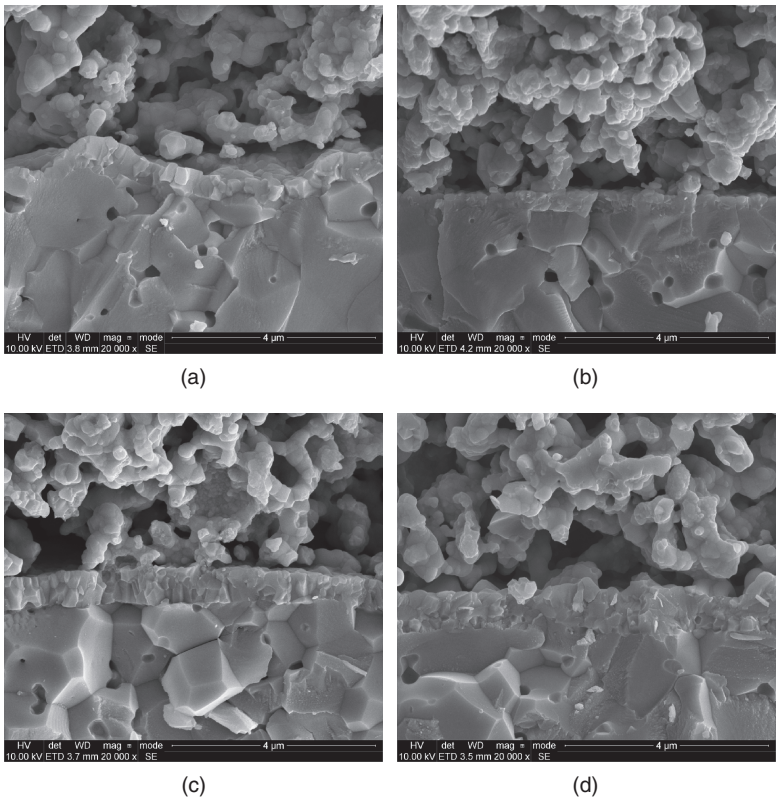

Fig. 2. SEM images of cathode-electrolyte interface for the structures without CGO layer (a) and with 400 nm (b), 800 nm (c) and 1200 nm (d) thick CGO layers.

deposition process can be noticed in the film layered microstructure. The CGO layers seem to be continuous and dense. For all investigated structures the LSF cathode had a highly porous microstructure.

An area specific resistance (ASR) obtained from the acquired impedance spectra was used as a measure of cathode–diffusion barrier–electrolyte interface performance. Typical Nyquist and Bode plots of impedance spectra for two- and three-electrode symmetrical configuration measurements collected at 800°C are presented in **Fig. 3**. At least two semicircles, one at high and one at low frequencies, can be distinguished in the Nyquist plot [see Fig. 3(a)]. It can be also reflected by the low and high frequency features visible in the Bode plots [see Fig. 3(b)]. However, depending on temperature and measurement configuration, the contribution of high and low frequency polarization resistance is not straight forward to analyze. Therefore, for simplicity and to avoid misinterpretations, only total polarization resistance was retrieved from the impedance spectra. The total polarization resistance was obtained by subtracting an ohmic resistance from a total resistance. An area specific resistance was calculated from polarization resistance taking into account a surface area of the electrode. In the case of the two-electrode configuration measurements, the results were divided by two to take into account two symmetrical interfaces. The ohmic resistance was not analyzed in this paper, since it resulted mostly from the ohmic resistance of YSZ electrolyte due to the fact that the CGO thickness is significantly smaller than the thickness of YSZ.

Figure 4 presents the polarization resistance as a function of temperature for all investigated structures, i.e. two-electrode symmetrical configuration, three-electrode symmetrical and three-electrode asymmetrical configuration. It can be seen that similar results were obtained for all investigated structures. **Figure 5** shows the results indicating the influence of the size of the electrode in a three-electrode symmetrical configuration on polarization resistance. It is evident that for the electrodes with a diameter below 0.9 cm the results are basically overlapping with each other, while for the electrode with a diameter of 0.9 cm the results differ significantly from the others. However, it needs to be noted that in the case of the 0.9 cm electrode diameter, the reference electrode was located at a shorter distance from the working electrode than triple the thickness of the electrolyte. This may lead to situation that the reference electrode potential is disturbed by the electrical current flowing between counter and working electrodes, which may lead to erroneous results.[14] Therefore, the size of the working and counter electrodes needs to properly selected.

In order to conclusively confirm that the polarization resistances obtained from the two-electrode and the three-electrode measurement configurations are the same, respective impedance spectra of the same sample need to be compared. Subsequently, asymmetrical structure with reference electrode was measured in two-electrode and three-electrode configuration, as shown in **Fig. 6**. In the case of the three-electrode configuration each of the interfaces, LSF and Pt, was measured separately. It is visible that the polarization resistance of Pt/YSZ interface has characteristic frequency of approximately 3 kHz [see Fig. 6(b)] and the shape of semicircle [see Fig. 6(a)]. Reaction kinetics of this interface is co-limited by oxygen adsorption and surface diffusion.[18] Impedance of LSF/YSZ interface is easily distinguishable as it can be modeled by at least two features [see Fig. 6(b)] connected with oxygen surface exchange in lower frequencies and interfacial resistance in higher frequencies.[20] The impedances of each interface were added for every frequency and as a result a new spectrum was obtained, which nearly exactly follow the results

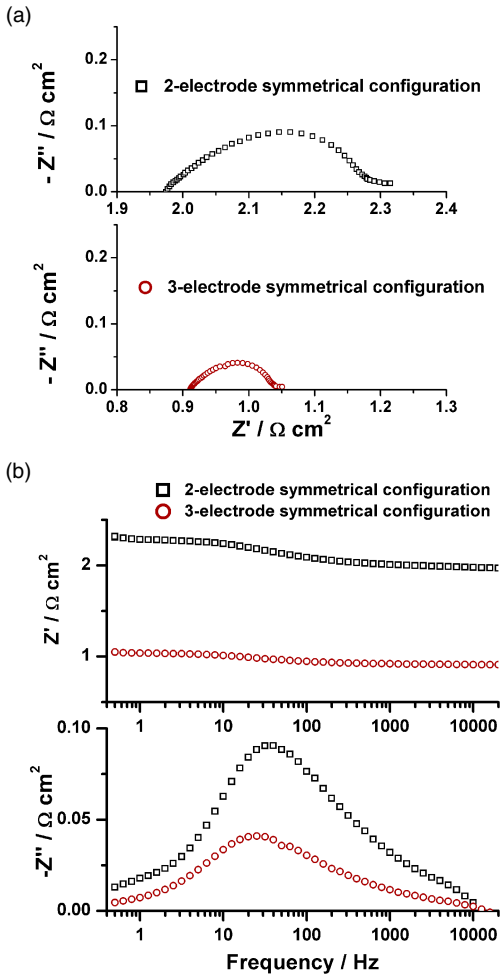

Fig. 3. Nyquist (a) and Bode (b) plots of impedance spectra for the two-electrode and three-electrode symmetrical configuration measurements collected at 800°C.

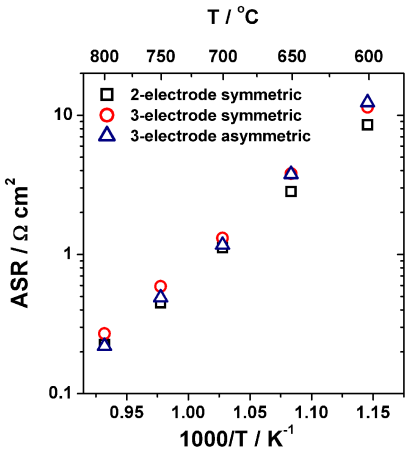

Fig. 4. Arrhenius plots of the area specific resistance for all measurement configurations.

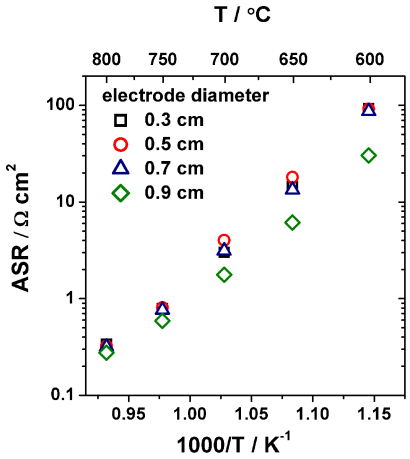

Fig. 5. Arrhenius plots of the area specific resistance for different diameters of the working and counter electrodes obtained for the three-electrode configuration measurements.

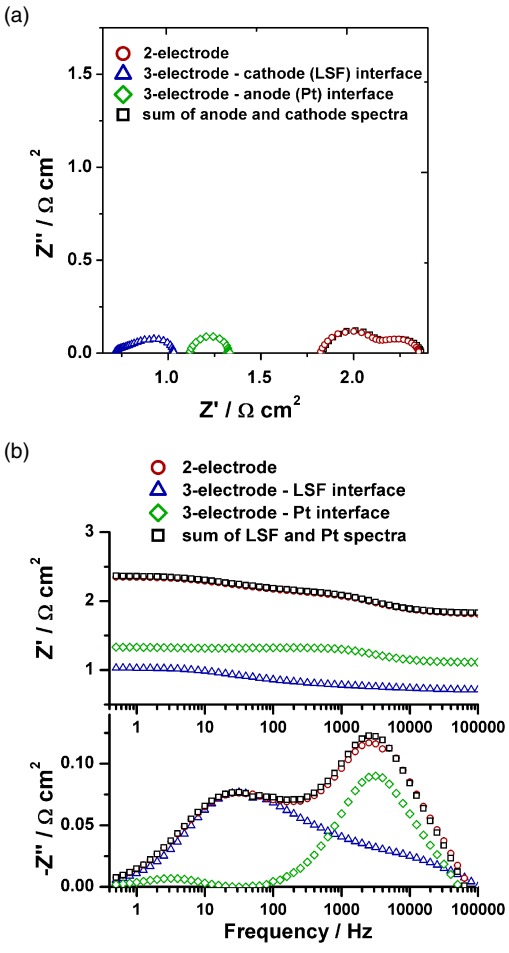

Fig. 6. Nyquist (a) and Bode (b) plots of impedance spectra for the two electrode measurements of the 3-electrode asymmetrical configuration sample, LSF and Pt interfaces of the 3-electrode asymmetrical configuration sample and the sum of the LSF and Pt interfaces collected at 800°C.

obtained for the two-electrode measurement. This illustrates the advantage of the three-electrode configuration method, which allows separating the contribution of the individual interfaces of investigated structure. Therefore, the following results are based on data obtained from the 3-electrode asymmetrical configuration. One should note that it is easier to fabricate structures in this configuration, since it is necessary to deposit the CGO layer on one side of electrolyte only.

The temperature dependence of the area specific resistances measured for the structures with and without the CGO diffusion

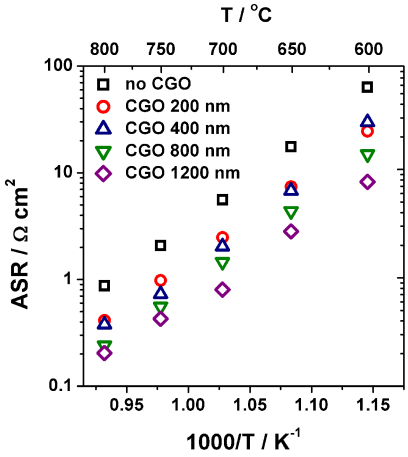

Fig. 7. Arrhenius plots of the area specific resistance for different thickness of the CGO diffusion barrier layer (electrodes diameter 0.7 cm).

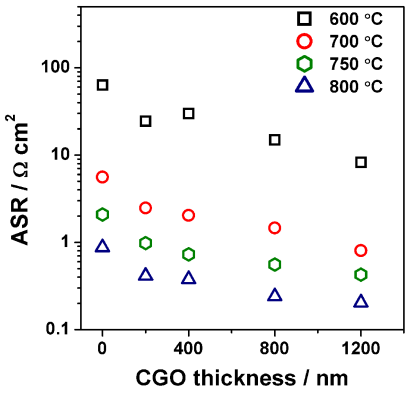

Fig. 8. The area specific resistance as a function of thickness of the CGO diffusion barrier layer at selected temperatures.

barrier layer is shown in **Fig. 7**. In the case of the structures with CGO layer, the thickness of CGO layer was altered from 400 nm up to 1200 nm. It is evident that with the introduction and increase of the CGO diffusion barrier thickness the polarization resistances of the investigated structures decrease. The most significant decrease of the resistance was obtained once the CGO layer was introduced. The thicker is the CGO layer thickness, the lower is the resistance, but the decrease rate become milder, as illustrated in **Fig. 8**.

The three-electrode configuration measurements allow the determination of polarization resistance under applied bias voltage. This allows to simulate fuel cell operating conditions, i.e. estimation of polarization resistance for fuel cell operating under load. This possibility was used for assessing changes in the ASR with the CGO diffusion barrier layer in the range of bias from 0 to 0.2 V. Such a variation of the bias voltage reflects the conditions of cathode overpotentials observed during solid oxide fuel cell operation. The results of this investigation are depicted in **Fig. 9**. In the case of the structure without a CGO diffusion barrier layer, the increase of the polarization resistance with the increase of the bias voltage is clearly visible. For the structure under the bias voltage of 0.2 V, the polarization resistance is doubled in comparison to a structure without applied bias voltage. The introduction of CGO layer significantly undermines this process. In case of the structure with 1200 nm CGO layer thick, the change of polarization resistance for the unbiased and biased structure is nearly insignificant (less than 15% increase).

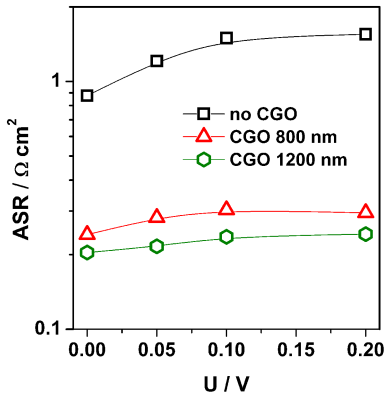

Fig. 9. The area specific resistance as a function of bias voltage for different thickness of the CGO diffusion barrier layer.

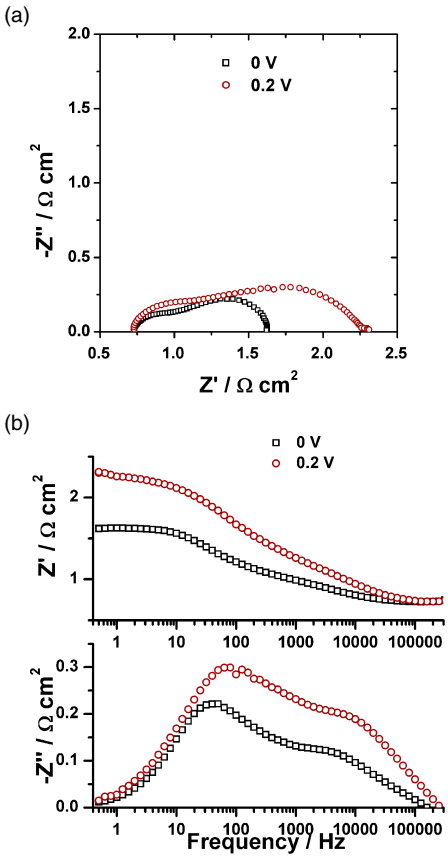

Fig. 10. Nyquist (a) and Bode (b) plots of impedance spectra of the sample without CGO barrier layer measured at a bias voltage of 0 and 0.2 V collected at 800°C.

Explanation of this phenomenon must be sought in the impedance spectrum shown in **Fig. 10**, in which the impedance spectra for the structure without CGO layer measured under a bias voltage of 0 and 0.2 V is presented. As expected, the ohmic resistance is unaffected by the bias voltage [see Fig. 10(a)]. It can be noticed that the increase of polarization resistance is manifested by the increase of the high- and the low-frequency features [see Fig. 10(b)]. The increase of the high-frequency feature is similar to the increase reported in.[20] The low-frequency feature can be attributed to surface exchange or diffusion limitation processes. Indeed, once the parasitic layer of strontium-zirconate is formed,

the surface exchange process can be limited, especially at the higher oxygen demand condition (under bias). On the other hand at the higher oxygen demand the diffusion limited process can also be expected. However, the diffusion limited process in fuel cell operation condition occur at the higher overpotentials and it is usually attributed to a water formed, which block electro-active sides in a anode. It seems that more research needs to be performed to conclusively describe this feature. Nevertheless, this may suggest that the bias voltage allows perceiving an increased polarization resistance, which is not so visible in case of the unbiased measurement conditions. It appears that a significant effect in this process may play a strontium-zirconate phase formed during the sintering of the LSF cathode in contact with the YSZ electrolyte [see Fig. 2(a)]. The introduction of the CGO diffusion barrier layer significantly reduces the polarization resistance, which is more apparent when measurements are performed in 3-electrode configuration with bias voltage.

4. Conclusions

It was shown that three-electrode configuration measurements provide reliable results if the reference electrode was placed sufficiently far away from the working and counter electrodes. Using this technique it is possible to separate the contribution of the individual interfaces of investigated structure. Moreover, the preparation of structures for electrical evaluation, especially for structures with multi-layer interfaces, is significantly simplified in comparison to structures for the two-electrode symmetrical configuration measurements, since it is necessary to fabricate investigated interfaces on one side of electrolyte only. Additionally, three-electrode configuration allows measuring and observing processes of the investigated interface under voltage bias what simulates fuel cell conditions operated under load. The three-electrode configuration was used in this paper to investigate the influence of CGO diffusion barrier layer thickness on polarization resistance of cathode/doped ceria diffusion barrier/doped zirconia electrolyte. The CGO diffusion barrier layer was fabricated by spray pyrolysis methods. It was shown that the polarization resistance was reduced when CGO diffusion barrier layer was introduced. The introduction of 1200 nm thick CGO layer lead to a fivefold reduction in the ASR at 800°C. Moreover, the introduction of the CGO layer lowered the growth of the polarization resistance visible in the presence of the bias voltage.

Acknowledgments This work is partly supported by project founded by National Science Centre Poland based on decision DEC-2012/05/B/ST7/02153.

References

1) S. Banerjee and A. K. Tyagi, Functional Materials. Preparation, Processing and Applications, ELSEVIER (2012) s 669-670, ISBN: 978-0-12-385142-0.
2) R. K. Akikur, R. Saidur, H. W. Ping and K. R. Ullah, *Energy Convers. Manage.*, **79**, 415–430 (2014).
3) A. Dutta, J. Mukhopadhyay and R. N. Basu, *J. Eur. Ceram. Soc.*, **29**, 2003–2011 (2009).
4) J. W. Lee, Z. Liu, L. Yang, H. Abernathy, S. H. Choi, H. E. Kim and M. Liu, *J. Power Sources*, **190**, 307–310 (2009).
5) G. C. Kostogloudis, G. Tsiniarakis and Ch. Ftikos, *Solid State Ionics*, **135**, 529–535 (2000).
6) M. Sase, D. Ueno, K. Yashiro, A. Kaimai, T. Kawada and J. Mizusaki, *J. Phys. Chem. Solids*, **66**, 343–348 (2005).
7) F. W. Poulsen and N. van der Puil, *Solid State Ionics*, **53–56**, 777–783 (1992).
8) G. Constantin, C. Rossignol, J.-P. Barnes and E. Djurado, *Solid State Ionics*, **235**, 36–41 (2013).
9) P. Plonczak, M. Joost, J. Hjelm, M. Sřgaard, M. Lundberg and P. V. Hendriksen, *J. Power Sources*, **196**, 1156–1162 (2011).
10) V. V. Krishnan, S. McIntosh, R. J. Gorte and J. M. Vohs, *Solid State Ionics*, **166**, 191–197 (2004).
11) M. J. Jørgensen and M. Mogensen, *J. Electrochem. Soc.*, **148**, A433–A442 (2001).
12) S. P. Jiang, *J. Appl. Electrochem.*, **34**, 1045–1055 (2004).
13) J. Rutman and I. Riess, *Electrochim. Acta*, **52**, 6073–6083 (2007).
14) S. B. Adler, B. T. Henderson, M. A. Wilson, D. M. Taylor and R. E. Richards, *Solid State Ionics*, **134**, 35–42 (2000).
15) M. Cimenti, A. C. Co, V. I. Briss and J. M. Hill, *Fuel Cells (Weinheim, Ger.)*, **5**, 364–376 (2007).
16) Z. Liu, J. S. Wainright, W. Huang and R.F. Savinell, *Electrochim. Acta*, **49**, 923–935 (2004).
17) G. J. Offer, P. Shearing, J. I. Golbert, D. J. L. Brett, A. Atkinson and N. P. Brandon, *Electrochim. Acta*, **53**, 7614–7621 (2008).
18) S. B. Adler, *Chem. Rev.*, **104**, 4791–4843 (2004).
19) M. Nagata, Y. Itoh and H. Iwahara, *Solid State Ionics*, **67**, 215–224 (1994).
20) F. S. Baumann, J. Fleig, H.-U. Habermeier and J. Maier, *Solid State Ionics*, **177**, 1071–1081 (2006).